Applied Mathematics and Computation 468 (2024) 128526

Contents lists available at ScienceDirect

Applied Mathematics and Computation

journal homepage: www.elsevier.com/locate/amc

On the exact and population bi-dimensional reproduction numbers in a stochastic SVIR model with imperfect vaccine

Gamboa M. [a,*], López-García M. [b], Lopez-Herrero M.J. [a]

[a] Faculty of Statistical Studies, Complutense University of Madrid, Madrid, 28040, Spain
[b] School of Mathematics, University of Leeds, Leeds, LS2 9JT, United Kingdom

ARTICLE INFO

MSC:
92D30
60J28
60J22

Keywords:
Stochastic epidemic model
Markov chain
Basic reproduction number
Imperfect vaccine

ABSTRACT

We aim to quantify the spread of a direct contact infectious disease that confers permanent immunity after recovery, within a non-isolated finite and homogeneous population. Prior to the onset of the infection and to prevent the spread of this disease, a proportion of individuals was vaccinated. But the administered vaccine is imperfect and can fail, which implies that some vaccinated individuals get the infection when being in contact with infectious individuals. We study the evolution of the epidemic process over time in terms of a continuous-time Markov chain, which represents a general SIR model with an additional compartment for vaccinated individuals. In our stochastic framework, we study two bi-dimensional variables recording infection events, produced by a single infectious individual or by the whole infected group, taking into account if the newly infected individual was previously vaccinated or not. Theoretical schemes and recursive algorithms are derived in order to compute joint probability mass functions and factorial moments for these random variables. We illustrate the applicability of our techniques by means of a set of numerical experiments.

1. Introduction

Outbreaks of infectious diseases have been almost constant throughout history, killing millions of individuals around the world. For example, the Black Death, also known as the Plague, was a bubonic plague pandemic that struck Europe and Asia in the mid-1300s. It killed around 200 million people and is considered the deadliest pandemic in human history. In 1520, another devastating pandemic was caused by smallpox. Although the origin of this disease is unknown, there is evidence of its existence at a very early time, since remains have been found in Egyptian mummies dating from the third century BC [1]. Even in the modern era, epidemic outbreaks are a serious threat to public health. SARS, MERS, avian influenza, Ebola and COVID-19 epidemics, among others, have reminded the world of the risk associated with infectious diseases outbreaks and of the importance of improving knowledge of the dynamics of disease spread in order to develop control strategies to stop or reduce transmission.

Vaccination is one of the most powerful tools to prevent infectious diseases. Vaccines can provide immunity against a disease, by helping the immune system to recognize the pathogen that causes the infection, without the need for the host to be exposed to it. Over the last two centuries, vaccination has enabled smallpox to be eradicated, it has reduced global child mortality rates preventing countless birth defects and lifelong disabilities [2,3]. However, lifelong protection is not always guaranteed by vaccines,

* Corresponding author.
E-mail address: mgamboa@ucm.es (M. Gamboa).

https://doi.org/10.1016/j.amc.2023.128526
Received 12 June 2023; Received in revised form 28 November 2023; Accepted 27 December 2023

Available online 5 January 2024
0096-3003/© 2024 The Authors. Published by Elsevier Inc. This is an open access article under the CC BY-NC-ND license (http://creativecommons.org/licenses/by-nc-nd/4.0/).

and the duration of protection against a given pathogen depends both on the type of infectious agent and the type of vaccine. In some occasions, several doses are necessary to guarantee immunity in the long-term, and even vaccine boosters or constant pulse vaccination programs in the population are required for some pathogens [4–6]. In other occasions, as it is assumed in this work, vaccines are imperfect and some vaccinated individuals eventually become infected after being exposed to the corresponding pathogen [7].

As vaccination is an effective method to prevent the spread of infection, mathematical compartmental epidemic models, with or without a specific vaccination compartment, have been developed to study the efficacy of vaccination strategies to control relevant diseases. Typically, the interest is in studying the efficacy of different vaccination strategies for certain relevant diseases [8–14]. In the literature, some papers deal with compartmental epidemic models assuming 100% perfect vaccines [15–20] but many others consider vaccines that are imperfect, and where vaccinated individuals can be infected by the infectious pathogen with a certain probability [21–23].

Under the imperfect vaccine hypothesis, SIS and SIR models have been analyzed from a deterministic approach [24,25], but also from a stochastic one. In more detail, an SIS model with imperfect vaccine is studied following a stochastic approach in [26,27]. In [4,28], authors study a stochastic SIS model with external source of infection and quantify the efficacy of several preventive measures surrounding vaccination. For a closed population, authors in [29], study the stationary distribution in a stochastic SVIR-type model. In [30], the length of an outbreak is studied for a non-linear incidence rate model and in [31], a latency period is included in the model.

In [32], we introduced an SVIR model with an external source of infection and imperfect vaccine, and we studied the time to reach a total number M of infections, in order to quantify timescales for disease spread. In the present paper, we plan to extend the study initiated in [32] to measure the potential transmission of the infectious disease, in terms of alternative quantities to the basic reproduction number, R_0, or the control reproduction number, R_c, that record the expected number of individuals that a single infectious one is able to infect either with or without control measures, respectively [34–38].

When we are dealing with small to moderate-sized populations (such as hospitals, schools or prisons), the basic reproduction and the control numbers tend to overestimate the real number of infections caused by a single individual while infectious. In stochastic Markovian models, we can correct this excess by focusing on exact and population reproduction numbers R_{e0} and R_p [28,33]. These random variables provide exact measures to quantify the expansion of an epidemic process and present an interesting property: they can be defined at all times and not only at the time of invasion, when the typical infectious individual is introduced into a completely susceptible population.

Hence, we reformulate the treatment of R_{e0} and R_p initiated in [28,33], for evaluating infection spread in our stochastic SVIR model. This refinement consists of analyzing the above stochastic measures in terms of two different contributions each, by distinguishing between infections caused across either susceptible or vaccinated pools of individuals. In this way, one can better understand the contribution that susceptible and vaccinated individuals play in the overall transmission through the corresponding reproduction numbers.

The rest of the paper is organized as follows. Section 2 contains the description of the stochastic SVIR model with an external source of infection and imperfect vaccine. In Sections 3 and 4, we define and analyse the random variables R_{e0} and R_p, and split them into two different contributions to account for the type of individuals becoming infected (i.e., either if they are vaccinated or not). Section 5 contains a set of numerical experiments to illustrate our techniques, while concluding remarks are given in Section 6.

2. Model description

We consider a non-isolated homogeneously mixed finite and constant size population, where an infectious disease is spreading. The pathogen is transmitted by direct contact with infected individuals, who acquire natural and long-life immunity once recovered. To model the evolution of the epidemic we consider the stochastic Susceptible-Vaccinated-Infected-Recovered (*SVIR*) type model introduced in [32]. Thus, individuals are classified as susceptible (S), vaccinated (V), infected (I) or recovered (R).

As the population is not isolated, infections occur through direct contact with infected individuals either inside or outside the population. Within the population and during their infectious period, any infected individual contacts susceptible ones following a time-homogeneous Poisson process with rate β; additional to this, there is another Poisson flow, of infection rate ξ, representing contacts with external infectious individuals.

As a control measure, we consider that a proportion of the population has received a vaccine against the underlying contagious disease. However, the administered vaccine is not perfect and there is a risk that a vaccinated individual develops the disease. So, we denote by h the probability that a vaccinated individual can be infected after exposed to the pathogen. We assume that, no matter if they were previously vaccinated or not, all infected individuals develop immunity after recovery, which takes an exponentially distributed time with rate γ.

Changes in health state imply movement of individuals among compartments in the model. Fig. 1 is a schematic diagram representing these changes.

For $t \geq 0$, let $V(t)$, $S(t)$, $I(t)$ and $R(t)$ represent the number of vaccinated, susceptible, infected and recovered individuals, respectively. Since we consider a constant size population, all these variables are linked as $V(t) + S(t) + I(t) + R(t) = N$, where N is the total population size. Hence, the evolution on the number of individuals in each compartment is represented by the following three-dimensional CTMC

$$\mathcal{X} = \{X(t) = (V(t), S(t), I(t)) : t \geq 0\}.$$

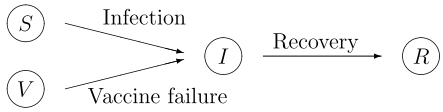

Fig. 1. Transitions between compartments in the SVIR model.

To describe its state space we assume, without loss of generality, that at $t = 0$ there are not recovered individuals. So, the initial state is expressed as $X(0) = (V(0), S(0), I(0)) = (v_0, s_0, N - v_0 - s_0)$, for integers v_0 and s_0 such that $0 \le v_0 + s_0 \le N$, and the state space of $\mathcal{X}$ is

$$\mathsf{S} = \{(v, s, i) : 0 \le v \le v_0, 0 \le s \le s_0, 0 \le v + s + i \le N\}. \tag{1}$$

The dynamics of the epidemic over time is directly related to transitions of $\mathcal{X}$ across states in S. In particular, given a state $(v, s, i) \in \mathsf{S}$, the following three events can occur: (a) An infected individual contacts a susceptible one who becomes infected; which occurs with rate

$$\lambda_{s,i} = \left(\frac{\beta i}{N} + \xi\right) s. \tag{2}$$

(b) Due to a vaccine failure, the contact between an infectious and a vaccinated individual results in a new case of infection; which occurs with rate

$$\eta_{v,i} = h\left(\frac{\beta i}{N} + \xi\right) v. \tag{3}$$

(c) An infected individual recovers; this occurs with rate

$$\gamma_i = \gamma i.$$

Summarizing, the infinitesimal transition rates of $\mathcal{X}$ are given by

$$q_{(v,s,i),(v^*,s^*,i^*)} = \begin{cases} \eta_{v,i} & \text{if } (v^*, s^*, i^*) = (v-1, s, i+1), \\ \gamma_i, & \text{if } (v^*, s^*, i^*) = (v, s, i-1), \\ -q_{v,s,i}, & \text{if } (v^*, s^*, i^*) = (v, s, i), \\ \lambda_{s,i}, & \text{if } (v^*, s^*, i^*) = (v, s-1, i+1), \\ 0, & \text{otherwise}, \end{cases} \tag{4}$$

where $q_{v,s,i} = \eta_{v,i} + \lambda_{s,i} + \gamma_i$, with $q^{-1}_{v,s,i}$ representing the average sojourn time spent at each state $(v, s, i) \in \mathsf{S}$.

To develop the analysis of variables appearing in the following sections we are going to use the division in levels and sublevels of the state space S described in [32], which leads us to represent the infinitesimal generator of the Markov chain in a block-tridiagonal form associated to a Quasi Birth-and-Death (*QBD*) process. That is,

$$\mathsf{S} = \cup_{v=0}^{v_0} l(v),$$

where $l(v) = \cup_{s=0}^{s_0} l(v, s)$, for $0 \le v \le v_0$, and $l(v, s) = \{(v, s, i) \in \mathsf{S} : \ 0 \le i \le N - v - s\}$, for $0 \le s \le s_0$.

As we stated in [32], when $\xi > 0$ the external flow of infections makes that disease can appear in a population where no infectious individuals are present. In that case, we are dealing with a finite state Markov chain that contains a single absorbing state, $(0, 0, 0)$, representing a population where all individuals have been recovered from the disease. Therefore, the theory of finite CTMCs ensures that, in the long-term, the stochastic process will become absorbed into this state in a finite time with probability one, and the expected time to absorption is finite. This asymptotic theoretical result means that the disease will affect the whole population during a finite, but not necessarily short, expected time.

But even though the outbreak is expected to end in a finite time, first stages of the epidemic process are crucial to adopt sanitary or disease containment measures. Hence, the study of transmission of the infectious disease from a single individual or from a controlled group of infectious individuals will be the subject matter of following sections.

3. The bi-dimensional exact transmission number, (R^V_{e0}, R^S_{e0})

In this section we will study the number of infections caused by a single infectious individual, affecting either susceptible or vaccinated individuals. We typically consider initial states where the infectious individual is the one starting the outbreak, called patient zero or index case in an epidemiological context, although our calculations require computing these stochastic descriptors for more general initial states.

Authors in [33,39] present, for stochastic Markovian models, two different approaches to evaluate the probability mass function of the number of secondary infections caused directly from the index case. In the present study, we will take the advantage of the approach described in [33] to derive systems of linear equations, whose solution can be computed using stable recursive procedures

suitable to handle large state spaces, as the ones considered in the illustrative examples in Section 5. The novel approach of our present work is to distinguish between transmission to susceptible and vaccinated individuals when analysing this measure.

Obviously, infection transmission depends on the initial size of the susceptible and vaccinated groups. Assuming that the outbreak starts from a state $(v_0, s_0, 1)$, with $v_0 + s_0 = N - 1$, to lighten notation, we omit references to initial state and simply write R^V_{e0} and R^S_{e0} to describe the number of vaccinated or susceptible individuals, respectively, directly infected by the index case, until he/she recovers.

We notice that a measure of the spread of the epidemic process in the entire population can be recorded from these variables as

$$R_{e0} = R^V_{e0} + R^S_{e0}, \tag{5}$$

whose expected value provides a stochastic analogue of the control reproduction number, R_c, that considers vaccination as a control measure.

To study the bidimensional random vector (R^V_{e0}, R^S_{e0}), we mark the index case and count the number of infections caused by him/her during his/her infectious period. The CTMC evolves in the following subset of the state space

$$\widehat{\mathsf{S}} = \{(v, s, i) \in \mathsf{S} : \ 1 \le i \le N - v - s\}.$$

We can decompose contagion rates in Eq. (2) and Eq. (3) by distinguishing between secondary cases caused by the index case or from other infectious individuals, if any. More specifically, we have

$$\lambda_{s,i} = \lambda^*_s + \widetilde{\lambda}_{s,i},$$
$$\eta_{v,i} = \eta^*_v + \widetilde{\eta}_{v,i},$$

where

$$\eta^*_v = h\frac{\beta}{N}v, \widetilde{\eta}_{v,i} = h\left(\frac{\beta(i-1)}{N} + \xi\right)v,$$
$$\lambda^*_s = \frac{\beta}{N}s, \widetilde{\lambda}_{s,i} = \left(\frac{\beta(i-1)}{N} + \xi\right)s.$$

As we are dealing with an infectious disease that confers permanent immunity taking place in a constant finite size population, the maximum number of infections produced by the index case can be at most of v_0 vaccinated and s_0 susceptible individuals. Thus, R^V_{e0} and R^S_{e0} have finite supports.

To study the joint distribution we focus on probability mass and generating functions, and factorial moments of the bi-dimensional random vector (R^V_{e0}, R^S_{e0}), conditioned to the initial state $(v_0, s_0, 1)$. As the CTMC evolves in time, the current state of the process changes at each transition. Therefore, we introduce general probability and generating functions, and moments for (R^V_{e0}, R^S_{e0}), conditioned to any state $(v, s, i) \in \widehat{\mathsf{S}}$, representing the current state of the CTMC at any given time. We point out that these random variables record the number of new cases of infection, within the susceptible and vaccinated pools, which take place during the infectious period of the marked infectious individual.

We can obtain recursive schemes whose solution will provide the desired descriptor (i.e., mass probability, generating function and moments) for the particular initial state $X(0) = (v_0, s_0, 1)$ of interest. In particular, we define

$$\begin{aligned}
x^{l,k}_{v,s,i} &= P\left\{R^V_{e0} = l, R^S_{e0} = k \,|X(0) = (v, s, i)\right\}, \text{ for } 0 \le l \le v, 0 \le k \le s,\\
\varphi^{V,S}_{v,s,i}(z, w) &= E\left[z^{R^V_{e0}} w^{R^S_{e0}} \,|X(0) = (v, s, i)\right],\\
&= \sum_{r=0}^{v}\sum_{j=0}^{s} z^r w^j P\left\{R^V_{e0} = r, R^S_{e0} = j \,|X(0) = (v, s, i)\right\},\\
&\quad \text{for } |z| \le 1, |w| \le 1,\\
m^{l,k}_{v,s,i} &= E\left[\Pi^{l-1}_{r=0}(R^V_{e0} - r)\Pi^{k-1}_{j=0}(R^S_{e0} - j) \,|X(0) = (v, s, i)\right], \text{ for } l, k \ge 0,
\end{aligned}$$

where empty products are considered to be equal to 1 here and in what follows.

To derive the mass probability distribution of (R^V_{e0}, R^S_{e0}), first we consider some basic features of these random variables conditioned to $(v, s, i) \in \widehat{\mathsf{S}}$. First, we notice that due to the support of this random vector being finite, we have

$$P\{R^V_{e0} < +\infty, R^S_{e0} < +\infty \,|X(0) = (v, s, i)\} = 1. \tag{6}$$

Consequently, $\sum_{l=0}^{v}\sum_{k=0}^{s} x^{l,k}_{v,s,i} = 1$, for any initial state $(v, s, i) \in \widehat{\mathsf{S}}$. Moreover, it is clear that

$$x^{l,k}_{v,s,i} = 0, \text{ for } l > v \text{ and/or } k > s. \tag{7}$$

Finally, when all individuals are either infectious or recovered, new contagions are not possible, so that for $1 \le i \le N$ we obtain the following boundary conditions

$$x^{0,0}_{0,0,i} = 1. \tag{8}$$

Next, we need to introduce some notation. For any number of vaccinated and susceptible individuals with $0 \le v \le v_0$ and $0 \le s \le s_0$, and integers $l, k \ge 0$, we denote

$$\mathbf{x}^{l,k}_{v,s} = (x^{l,k}_{v,s,1}, \dots, x^{l,k}_{v,s,N-v-s})^T,$$
$$\widehat{\mathbf{x}}^{l,k}_{v,s} = (x^{l,k}_{v,s,2}, \dots, x^{l,k}_{v,s,N-v-s})^T.$$

In what follows, $\mathbf{1}_j$ and $\mathbf{0}_j$ will represent j-dimensional all-ones and all-zeroes column vectors, respectively. We also denote $\mathbf{\Gamma}_j = \gamma \mathbf{1}_j$.

Theorem 1 shows how the organisation by levels and sub-levels of the state space of the Markov chain, $\mathcal{X}$, allows us to obtain block-diagonal structured matrices which facilitate the computation of the linear systems of equations that need to be solved in order to compute the desired probabilities $x^{l,k}_{v,s,i}$.

Theorem 1. *For any level $l(v)$, $0 \le v \le v_0$, sub-level $l(v,s)$, $0 \le s \le s_0$ and integers $l, k \ge 0$, joint probability mass functions of the conditioned random vector (R^V_{e0}, R^S_{e0}) can be computed as the solution of the following system of linear equations:*

$$\mathbf{x}^{0,0}_{0,0} = \mathbf{1}_N, \tag{9}$$

$$\mathbf{x}^{l,k}_{v,s} = \mathbf{0}_{N-v-s}, \text{ for } l > v \text{ and/or } k > s, \tag{10}$$

$$\begin{aligned}\mathbf{A}_{v,s}\mathbf{x}^{l,k}_{v,s} &= \delta_{l,0}\delta_{k,0}\mathbf{\Gamma}_{N-v-s} + (1-\delta_{v,0})\left((1-\delta_{l,0})\eta^*_v \widehat{\mathbf{x}}^{l-1,k}_{v-1,s} + \widetilde{\mathbf{E}}_{v,s}\widehat{\mathbf{x}}^{l,k}_{v-1,s}\right)\\ &\quad + (1-\delta_{s,0})\left((1-\delta_{k,0})\lambda^*_s \widehat{\mathbf{x}}^{l,k-1}_{v,s-1} + \widetilde{\mathbf{D}}_{v,s}\widehat{\mathbf{x}}^{l,k}_{v,s-1}\right),\end{aligned} \tag{11}$$

where $\delta_{a,b}$ denotes, here and in what follows, the Kronecker's delta function which takes the value 1 if $a = b$, and 0 otherwise. Matrices appearing in Equations (9)-(11) are described as follows: $\mathbf{A}_{v,s}$ is a bi-diagonal square matrix of dimension $N - v - s$ with non-null entries given by

$$\mathbf{A}_{v,s}(i,j) = \begin{cases} -(i-1)\gamma, & \text{if } j = i-1 \text{ and } 2 \le i \le N-v,\\ q_{v,s,i}, & \text{if } j = i \text{ and } 1 \le i \le N-v.\end{cases}$$

Diagonal matrices $\widetilde{\mathbf{D}}_{v,s}$ and $\widetilde{\mathbf{E}}_{v,s}$ have dimension $(N - v - s)$, with non-null diagonal elements given by $\widetilde{\mathbf{D}}_{v,s}(i,i) = \widetilde{\lambda}_{s,i}$, and $\widetilde{\mathbf{E}}_{v,s}(i,i) = \widetilde{\eta}_{v,i}$, for any $1 \le i \le N - v - s$.

Proof. We note that Equations (9) and (10) are the matrix version of Equations (8) and (7), respectively. For a given initial state, and conditioning on the first transition, we get the following relationship among probabilities of the conditioned bi-dimensional random vector

$$\begin{aligned}x^{l,k}_{v,s,i} &= \delta_{l,0}\delta_{k,0}\frac{\gamma}{q_{v,s,i}} + (1-\delta_{v,0})\left((1-\delta_{l,0})\frac{\eta^*_v}{q_{v,s,i}}x^{l-1,k}_{v-1,s,i+1} + \frac{\widetilde{\eta}_{v,i}}{q_{v,s,i}}x^{l,k}_{v-1,s,i+1}\right)\\ &\quad + (1-\delta_{s,0})\left((1-\delta_{k,0})\frac{\lambda^*_s}{q_{v,s,i}}x^{l,k-1}_{v,s-1,i+1} + \frac{\widetilde{\lambda}_{s,i}}{q_{v,s,i}}x^{l,k}_{v,s-1,i+1}\right)\\ &\quad + (1-\delta_{i,1})(i-1)\frac{\gamma}{q_{v,s,i}}x^{l,k}_{v,s,i-1}.\end{aligned} \tag{12}$$

Equation (12) is equivalent to

$$\begin{aligned}&-(1-\delta_{i,1})(i-1)\gamma x^{l,k}_{v,s,i-1} + q_{v,s,i}x^{l,k}_{v,s,i} =\\ &+\delta_{l,0}\delta_{k,0}\gamma + (1-\delta_{v,0})\left((1-\delta_{l,0})\eta^*_v x^{l-1,k}_{v-1,s,i+1} + \widetilde{\eta}_{v,i}x^{l,k}_{v-1,s,i+1}\right)\\ &+(1-\delta_{s,0})\left((1-\delta_{k,0})\lambda^*_s x^{l,k-1}_{v,s-1,i+1} + \widetilde{\lambda}_{s,i}x^{l,k}_{v,s-1,i+1}\right).\end{aligned} \tag{13}$$

For $1 \le i \le N - v - s$, Equation (11) is the matrix form representation of Equation (13), which completes the proof. □

The *loop-free* structure of the transition events of the continuous Markov chain (see Fig. 1) allows one to compute joint probability mass functions by solving the equations in Theorem 1 in an efficient and ordered way, via Algorithm 1. In particular, one starts from the boundary conditions (9) and (10), and applies the following expression derived from Equation (11):

$$\begin{aligned}\mathbf{x}^{l,k}_{v,s} &= (\mathbf{A}_{v,s})^{-1}\Bigg(\delta_{l,0}\delta_{k,0}\mathbf{\Gamma}_{N-v-s} + (1-\delta_{v,0})\left((1-\delta_{l,0})\eta^*_v\widehat{\mathbf{x}}^{l-1,k}_{v-1,s} + \widetilde{\mathbf{E}}_{v,s}\widehat{\mathbf{x}}^{l,k}_{v-1,s}\right)\\ &\quad + (1-\delta_{s,0})\left((1-\delta_{k,0})\lambda^*_s\widehat{\mathbf{x}}^{l,k-1}_{v,s-1} + \widetilde{\mathbf{D}}_{v,s}\widehat{\mathbf{x}}^{l,k}_{v,s-1}\right)\Bigg).\end{aligned} \tag{14}$$

Algorithm 1 Computation of the joint mass function of the vector (R^S_{e0}, R^V_{e0}), for any level $l(v)$, $0 \le v \le v_0$, sub-level $l(v,s)$, $0 \le s \le s_0$.

Input: N, v_0, s_0, β, ξ and γ.
Step 1: Set $k=0$, $l=0$, $v=0$ and $s=0$ and $\mathbf{x}^{0,0}_{v,s} = \mathbf{1}_{N-v-s}$.
Step 1a: Set $s=s+1$, compute $\mathbf{x}^{l,k}_{v,s}$ from (14).
Step 1b: If $s<s_0$, go to Step 1a.
Step 1c: Set $v=v+1$. If $v \le v_0$, set $s=-1$ and go to Step 1b.
Step 2: Set $l=l+1$.
Step 2a: Set $\mathbf{x}^{l,k}_{v,s} = \mathbf{0}_{N-v-s}$ for $0 \le v \le l-1$, $0 \le s \le s_0$.
Step 2b: Set $v=l$ and $s=0$.
Step 2c: Compute $\mathbf{x}^{l,k}_{v,s}$ from (14).
Step 2d: If $s<s_0$, set $s=s+1$ and go to Step 2c.
Step 2e: If $v<v_0$, set $v=v+1$, $s=0$ and go to Step 2c.
Step 2f: If $l<v_0$, go to Step 2.
Step 3: Set $k=k+1$ and $l=0$ and $v=0$.
Step 3a: Set $\mathbf{x}^{l,k}_{v,s} = \mathbf{0}_{N-v-s}$ for $0 \le s \le k-1$.
Step 3b: Set $s=k$.
Step 3c: Compute $\mathbf{x}^{l,k}_{v,s}$ from (14).
Step 3d: Set $s=s+1$, if $s<s_0$ go to step 3c.
Step 3e: If $v<v_0$, set $v=v+1$ and go to Step 3a.
Step 4: Set $l=l+1$.
Step 4a: Set $\mathbf{x}^{l,k}_{v,s} = \mathbf{0}_{N-v-s}$ for $0 \le v \le l-1$, $0 \le s \le s_0$.
Step 4b: Set $v=l$ and $s=k$.
Step 4c: Compute $\mathbf{x}^{l,k}_{v,s}$ from (14).
Step 4d: If $v<v_0$, set $v=v+1$ and go to step 4c.
Step 4e: If $l<v_0$, go to step 4.
Step 4f: If $k<s_0$ go to step 3.
Output: $\mathbf{x}^{l,k}_{v_0,s_0}$, *for* $0 \le k \le v_0$ *and* $0 \le l \le s_0$.

Next, we are interested in computing joint factorial moments of the conditioned random vector (R^V_{e0}, R^S_{e0}). Such moments could be obtained from the probability mass functions already computed. However, we propose here to obtain them more directly, through Theorem 2, with the help of joint gene-rating functions, $\varphi^{V,S}_{v,s,i}(z,w)$. This approach involves simpler expressions and therefore the algorithmic implementation is associated with shorter execution times. In particular, factorial moments can be obtained by applying the following property which involves their corresponding generating function, $\varphi^{V,S}_{v,s,i}(z,w)$, for $|z| \le 1, |w| \le 1$,

$$m^{l,k}_{v,s,i} = \left.\frac{\partial^{l+k}\varphi^{V,S}_{v,s,i}(z,w)}{\partial z^l \partial w^k}\right|_{w=1,z=1} \text{ for } l,k \ge 0. \tag{15}$$

We note that, due to the result shown in Equations (6) and (15), the following boundary condition is obtained

$$\varphi^{V,S}_{v,s,i}(1,1) = m^{0,0}_{v,s,i} = 1. \tag{16}$$

Directly by definition, we obtain the following marginal moments

$$m^{l,0}_{0,s,i} = 0, \text{ for } l>0, \tag{17}$$

$$m^{0,k}_{v,0,i} = 0, \text{ for } k>0. \tag{18}$$

In the absence of vaccinated and susceptible individuals within the population, the marked infectious individual cannot cause any infections. Thus, the following boundary condition is derived

$$m^{l,k}_{0,0,i} = 0, \text{ for } l,k>0. \tag{19}$$

Subsequently, we introduce the following notation that involves the mentioned factorial moments for any number of vaccinated and susceptible individuals, v and s, respectively, with $0 \le v \le v_0$, $0 \le s \le s_0$, and integers $l,k \ge 0$:

$$\mathbf{m}^{l,k}_{v,s} = (m^{l,k}_{v,s,1}, \dots, m^{l,k}_{v,s,N-v-s})^T,$$
$$\widehat{\mathbf{m}}^{l,k}_{v,s} = (m^{l,k}_{v,s,2}, \dots, m^{l,k}_{v,s,N-v-s})^T.$$

Theorem 2. *For any level $l(v)$, $0 \le v \le v_0$, sub-level $l(v,s)$, $0 \le s \le s_0$, and integers $l,k \ge 0$, the joint factorial moments of the conditioned random vector (R^V_{e0}, R^S_{e0}) can be computed as the solution of the following system of linear equations*

$$\mathbf{m}^{0,0}_{v,s} = \mathbf{1}_{N-v-s}, \tag{20}$$

$$\mathbf{m}^{l,0}_{0,s} = \mathbf{0}_{N-v-s}, \text{ for } l>0, \tag{21}$$

$$\mathbf{m}^{0,k}_{v,0} = \mathbf{0}_{N-v-s}, \text{ for } k>0, \tag{22}$$

$$\mathbf{m}^{l,k}_{0,0} = \mathbf{0}_{N}, \text{ for } l,k>0, \tag{23}$$

$$\mathbf{A}_{v,s}\mathbf{m}_{v,s}^{l,k} = (1-\delta_{v,0})\left(l\eta_v^*\widehat{\mathbf{m}}_{v-1,s}^{l-1,k} + \mathbf{E}_{v,s}\widehat{\mathbf{m}}_{v-1,s}^{l,k}\right) + (1-\delta_{s,0})\left(k\lambda_s^*\widehat{\mathbf{m}}_{v,s-1}^{l,k-1} + \mathbf{D}_{v,s}\widehat{\mathbf{m}}_{v,s-1}^{l,k}\right), \tag{24}$$

where matrices appearing in Equation (24) are described as follows: $\mathbf{A}_{v,s}$ *is defined in Theorem 1.* $\mathbf{D}_{v,s}$ *and* $\mathbf{E}_{v,s}$ *are diagonal matrices of dimension* $(N-v-s)$*, with non-null diagonal elements given by* $\mathbf{D}_{v,s}(i,i) = \lambda_{s,i}$*, and* $\mathbf{E}_{v,s}(i,i) = \eta_{v,i}$*, for any* $1 \le i \le N-v-s$*.*

Proof. For $1 \le i \le N-v-s$, Equation (20) is the matrix form representation of Equation (16). Equations (21)-(23) are the matrix version of Equations (17)-(19), respectively. Appealing to first-step arguments, we have that joint generating functions, $\varphi_{v,s,i}^{V,S}(z,w)$, of the conditioned vector (R_{e0}^V, R_{e0}^S) satisfy the following expressions for any $(v,s,i) \in \widehat{\mathbb{S}}$

$$\begin{aligned} q_{v,s,i}\varphi_{v,s,i}^{V,S}(z,w) = \gamma + (1-\delta_{v,0})\Big(\eta_v^* z\varphi_{v-1,s,i+1}^{V,S}(z,w) \\ + \widetilde{\eta}_{v,i}\varphi_{v-1,s,i+1}^{V,S}(z,w)\Big) + (1-\delta_{s,0})\Big(\lambda_s^* w\varphi_{v,s-1,i+1}^{V,S}(z,w) \\ + \widetilde{\lambda}_{s,i}\varphi_{v,s-1,i+1}^{V,S}(z,w)\Big) + (1-\delta_{i,1})\gamma(i-1)\varphi_{v,s,i-1}^{V,S}(z,w). \end{aligned} \tag{25}$$

By differentiating Equation (25) with respect to z repeatedly l times ($l \ge 1$) and to w repeatedly k times ($k \ge 1$), and evaluating at $z=1$ and $w=1$, we have the following system of equations for the factorial moments of (R_{e0}^V, R_{e0}^S) conditioned to state $(v,s,i) \in \widehat{\mathbb{S}}$:

$$\begin{aligned} q_{v,s,i}m_{v,s,i}^{l,k} = (1-\delta_{i,1})\gamma(i-1)m_{v,s,i-1}^{l,k} \\ + (1-\delta_{v,0})\left(l\eta_v^* m_{v-1,s,i+1}^{l-1,k} + \eta_{v,i}m_{v-1,s,i+1}^{l,k}\right) \\ + (1-\delta_{s,0})\left(k\lambda_s^* m_{v,s-1,i+1}^{l,k-1} + \lambda_{s,i}m_{v,s-1,i+1}^{l,k}\right). \end{aligned} \tag{26}$$

Equation (26) is equivalent to

$$\begin{aligned} -(1-\delta_{i,1})\gamma(i-1)m_{v,s,i-1}^{l,k} + q_{v,s,i}m_{v,s,i}^{l,k} = (1-\delta_{v,0})\Big(l\eta_v^* m_{v-1,s,i+1}^{l-1,k} \\ + \eta_{v,i}m_{v-1,s,i+1}^{l,k}\Big) + (1-\delta_{s,0})\left(k\lambda_s^* m_{v,s-1,i+1}^{l,k-1} + \lambda_{s,i}m_{v,s-1,i+1}^{l,k}\right), \end{aligned} \tag{27}$$

for $1 \le i \le N-v-s$, Equation (24) is its matrix representation, which completes the proof. □

Algorithm 2 allows us to compute the joint factorial moments of the conditioned random vector (R_{e0}^V, R_{e0}^S) in an iterative and ordered way. It exploits the following expression which is equivalent to Equation (24):

$$\begin{aligned} \mathbf{m}_{v,s}^{l,k} = (\mathbf{A}_{v,s})^{-1}\Big((1-\delta_{v,0})\left(l\eta_v^*\widehat{\mathbf{m}}_{v-1,s}^{l-1,k} + \mathbf{E}_{v,s}\widehat{\mathbf{m}}_{v-1,s}^{l,k}\right) \\ + (1-\delta_{s,0})\left(k\lambda_s^*\widehat{\mathbf{m}}_{v,s-1}^{l,k-1} + \mathbf{D}_{v,s}\widehat{\mathbf{m}}_{v,s-1}^{l,k}\right)\Big). \end{aligned} \tag{28}$$

Algorithm 2 Computation of the factorial moments of order $l_{max} \ge 0$ and $k_{max} \ge 0$ of the vector (R_{e0}^V, R_{e0}^S), for any level $l(v)$, $0 \le v \le v_0$, sub-level $l(v,s)$, $0 \le s \le s_0$.

Input: $N, v_0, s_0, \beta, \xi, \gamma, l_{max}$ and k_{max}.
Step 1: Set $k=0$, $l=0$ and $\mathbf{m}_{v,s}^{0,0} = \mathbf{1}_{N-v-s}$, for $0 \le v \le v_0$, $0 \le s \le s_0$.
Step 2: Set $l = l+1$, $v=0$ and $\mathbf{m}_{0,s}^{l,0} = \mathbf{0}_{N-v-s}$ for $0 \le s \le s_0$.
Step 3: set $v = v+1$, $s=0$ and compute $\mathbf{m}_{v,s}^{l,k}$ from (28).
    Step 3a: If $s < s_0$, set $s = s+1$ and compute $\mathbf{m}_{v,s}^{l,k}$ from (28) and go to Step 3a.
    Step 3b: If $v < v_0$, go to Step 3.
    Step 3c: If $l < l_{max}$, go to Step 2.
Step 4: Set $k = k+1$ and $l=0$.
    Step 4a: Set $v=0$.
    Step 4b: Set $s=0$, if $l=0$ or $v=0$ set $\mathbf{m}_{v,0}^{0,k} = \mathbf{0}_{N-v-s}$, else compute $\mathbf{m}_{v,s}^{l,k}$ from (28).
    Step 4c: If $s < s_0$, set $s = s+1$ and compute $\mathbf{m}_{v,s}^{l,k}$ from (28) and go to Step 4c.
    Step 4d: If $v < v_0$, set $v = v+1$ and go to Step 4b.
Step 5: If $l < l_{max}$, set $l = l+1$ and go to Step 4a.
Step 6: If $k < k_{max}$ go to Step 4.
Output: $\mathbf{m}_{v_0,s_0}^{l,k}$, *for* $0 \le k \le k_{max}$ *and* $0 \le l \le l_{max}$.

4. The bi-dimensional population transmission variable, (R_p^V, R_p^S)

An additional measure of the transmission capacity of the pathogen is R_p. This random variable counts the number of infections caused all infected individuals in the population (not just those directly caused by a marked individual) until the first recovery occurs [33].

Here, we also propose to characterize R_p while distinguishing between infections involving vaccinated and susceptible individuals, so that

$$R_p = R_p^V + R_p^S. \tag{29}$$

In particular, our aim is to characterize the joint distribution of the random vector (R_p^V, R_p^S), conditioned to an initial state $(v_0, s_0, N - v_0 - s_0)$.

To study this variable, we define the generating and probability mass functions of (R_p^V, R_p^S), and joint factorial moments of R_p^V and R_p^S, for any given initial state $(v, s, i) \in \widehat{\mathrm{S}}$, as

$$\begin{aligned}
X_{v,s,i}^{l,k} &= P\left\{ R_p^V = l, R_p^S = k \,|\, X(0) = (v,s,i) \right\}, \text{ for } 0 \le l \le v, 0 \le k \le s,\\
\phi_{v,s,i}^{V,S}(z,w) &= E\left[z^{R_p^V} w^{R_p^S} \,|\, X(0) = (v,s,i) \right]\\
&= \sum_{r=0}^{v} \sum_{j=0}^{s} w^j z^r P\left\{ R_p^V = r, R_p^S = j \,|\, X(0) = (v,s,i) \right\},\\
&\quad \text{for } |z| \le 1 \text{ and } |w| \le 1,\\
M_{v,s,i}^{l,k} &= E[\Pi_{r=0}^{l-1}(R_p^V - r)\Pi_{j=0}^{k-1}(R_p^S - j) \,|\, X(0) = (v,s,i)], \text{ for } l,k \ge 0.
\end{aligned}$$

We point out that both random variables have finite support. In particular, $0 \le R_p^V \le v_0$ and $0 \le R_p^S \le s_0$ and we have that

$$P\{ R_p^V < +\infty, R_p^S < +\infty \,|\, X(0) = (v,s,i) \} = 1. \tag{30}$$

Consequently, $\sum_{l=0}^{v} \sum_{k=0}^{s} X_{v,s,i}^{l,k} = 1$, for any initial state $(v, s, i) \in \widehat{\mathrm{S}}$. Moreover, when all individuals in the population are either infectious or recovered, new infections can not occur and in consequence

$$X_{0,0,i}^{0,0} = 1. \tag{31}$$

By definition, we also obtain the following boundary conditions

$$X_{v,s,i}^{l,k} = 0, \text{ for } l > v \text{ and/or } k > s. \tag{32}$$

We introduce the following notation for any number of vaccinated, v, and susceptible, s, individuals with $0 \le v \le v_0$, $0 \le s \le s_0$ and integers $l, k \ge 0$:

$$\begin{aligned}
\mathbf{X}_{v,s}^{l,k} &= (X_{v,s,1}^{l,k}, \ldots, X_{v,s,N-v-s}^{l,k})^T,\\
\widehat{\mathbf{X}}_{v,s}^{l,k} &= (X_{v,s,2}^{l,k}, \ldots, X_{v,s,N-v-s}^{l,k})^T.
\end{aligned}$$

Joint mass functions of the conditioned random variable (R_p^V, R_p^S) can be obtained applying Theorem 3.

Theorem 3. *For any level $l(v)$, $0 \le v \le v_0$, sub-level $l(v,s)$, $0 \le s \le s_0$ and integers $l, k \ge 0$, the joint probability mass functions of the conditioned random vector (R_p^V, R_p^S) can be computed as the solution of the following system of linear equations:*

$$\mathbf{X}_{0,0}^{0,0} = \mathbf{1}_N, \tag{33}$$

$$\mathbf{X}_{v,s}^{l,k} = \mathbf{0}_{N-v-s}, \text{ for } l > v \text{ and/or } k > s \tag{34}$$

$$\begin{aligned}
\widetilde{\mathbf{A}}_{v,s}\mathbf{X}_{v,s}^{l,k} &= \delta_{l,0}\delta_{k,0}\mathbf{\Gamma}_{N-v-s} + (1-\delta_{v,0})(1-\delta_{l,0})\mathbf{E}_{v,s}\widehat{\mathbf{X}}_{v-1,s}^{l-1,k}\\
&\quad + (1-\delta_{s,0})(1-\delta_{k,0})\mathbf{D}_{v,s}\widehat{\mathbf{X}}_{v,s-1}^{l,k-1},
\end{aligned} \tag{35}$$

where $\widetilde{\mathbf{A}}_{v,s}$ is a diagonal matrix of dimension $(N-v-s)$, with non-null diagonal elements given by $\widetilde{\mathbf{A}}_{v,s}(i,i) = q_{v,s,i}$ for any $1 \le i \le N-v-s$. Matrices $\mathbf{D}_{v,s}$ and $\mathbf{E}_{v,s}$ were defined in Theorem 2. $\mathbf{\Gamma}_{N-v-s}$ was defined in Theorem 1.

Proof. We point out that Equations (33) and (34) are the matrix version of Equations (31) and (32), respectively. For a given initial state, and conditioning on the first transition, the joint probability mass functions of the conditioned random vector (R_p^V, R_p^S) satisfy the following relationship

$$q_{v,s,i}X^{l,k}_{v,s,i} = \delta_{l,0}\delta_{k,0}\gamma i + (1-\delta_{l,0})(1-\delta_{v,0})\eta_{v,i}X^{l-1,k}_{v-1,s,i+1} + (1-\delta_{k,0})(1-\delta_{s,0})\lambda_{s,i}X^{l,k-1}_{v,s-1,i+1}. \tag{36}$$

For $1 \le i \le N-v-s$, Equation (35) is the matrix form representation of Equation (36), which concludes the proof. □

Remark 1. Mass functions of the bidimensional vector (R^V_p, R^S_p) can be computed from recursive schemes based on Theorem 3, and are the basis to obtain some of the numerical results in Section 5. The algorithmic computation is analogous to Algorithm 1, with the natural changes in notation and replacing Equation (14) by

$$\mathbf{X}^{l,k}_{v,s} = (\widetilde{\mathbf{A}}_{v,s})^{-1}\Big(\delta_{l,0}\delta_{k,0}\mathbf{\Gamma}_{N-v-s} + (1-\delta_{v,0})(1-\delta_{l,0})\mathbf{E}_{v,s}\widehat{\mathbf{X}}^{l-1,k}_{v-1,s} + (1-\delta_{s,0})(1-\delta_{k,0})\mathbf{D}_{v,s}\widehat{\mathbf{X}}^{l,k-1}_{v,s-1}\Big).$$

Similarly to the methodology employed in the preceding section, we derive factorial moments of the bidimensional random vector (R^V_p, R^S_p) conditioned to any state $(v,s,i) \in \widehat{\mathbb{S}}$ by using the generating function $\phi^{V,S}_{v,s,i}(z,w)$. From Equation (30), and by applying Equation (15), with the appropriate changes in notation, we obtain the following boundary condition

$$\phi^{V,S}_{v,s,i}(1,1) = M^{0,0}_{v,s,i} = 1. \tag{37}$$

By definition, marginal factorial moments $M^{l,0}_{0,s,i}$ and $M^{0,k}_{v,0,i}$ satisfy the following expressions

$$M^{l,0}_{0,s,i} = 0, \text{ for } l > 0, \tag{38}$$

$$M^{0,k}_{v,0,i} = 0, \text{ for } k > 0. \tag{39}$$

Moreover, when there are no vaccinated and susceptible individuals in the population, no infections can occur, and therefore we obtain the following boundary conditions

$$M^{l,k}_{0,0,i} = 0, \text{ for } l,k > 0. \tag{40}$$

Next we introduce some notation to derive the theoretical results involving factorial moments of the random variables of interest.

$$\mathbf{M}^{l,k}_{v,s} = (M^{l,k}_{v,s,1}, \dots, m^{l,k}_{v,s,N-v-s})^T,$$
$$\widehat{\mathbf{M}}^{l,k}_{v,s} = (m^{l,k}_{v,s,2}, \dots, m^{l,k}_{v,s,N-v-s})^T.$$

Theorem 4. *For any level $l(v)$, $0 \le v \le v_0$ and sub-level $l(v,s)$, $0 \le s \le s_0$, factorial moments of the conditioned random variable (R^V_p, R^S_p) can be computed as the solution of the following system of linear equations*

$$\mathbf{M}^{0,0}_{v,s} = \mathbf{1}_{N-v-s}, \text{ for } 0 \le v \le v_0, \tag{41}$$

$$\mathbf{M}^{l,0}_{0,s} = \mathbf{0}_{N-v-s}, \text{ for } l > 0, \tag{42}$$

$$\mathbf{M}^{0,k}_{v,0} = \mathbf{0}_{N-v-s}, \text{ for } k > 0, \tag{43}$$

$$\widetilde{\mathbf{A}}_{v,s}\mathbf{M}^{l,k}_{v,s} = (1-\delta_{s,0})\mathbf{D}_{v,s}\left(k\widehat{\mathbf{M}}^{l,k-1}_{v,s-1} + \widehat{\mathbf{M}}^{l,k}_{v,s-1}\right) + (1-\delta_{v,0})\mathbf{E}_{v,s}\left(l\widehat{\mathbf{M}}^{l-1,k}_{v-1,s} + \widehat{\mathbf{M}}^{l,k}_{v-1,s}\right), \tag{44}$$

where matrix $\widetilde{\mathbf{A}}_{v,s}$ was introduced in Theorem 3 and matrices $\mathbf{D}_{v,s}$ and $\mathbf{E}_{v,s}$ were described in Theorem 2.

Proof. For $1 \le i \le N-v-s$, Equation (41) is the matrix form representation of Equation (37). Equations (42)-(43) are the matrix version of Equations (38)-(39), respectively.

A first-step argument, conditioning on the possible transitions out of a state $(v,s,i) \in \widehat{\mathbb{S}}$, shows that the joint generating functions, $\phi^{V,S}_{v,s,i}(z,w)$, of (R^V_p, R^S_p) satisfy the following set of linear equations:

$$q_{v,s,i}\phi^{V,S}_{v,s,i}(z,w) = \gamma i + (1-\delta_{v,0})\eta_{v,i}z\phi^{V,S}_{v-1,s,i+1}(z,w) + (1-\delta_{s,0})\lambda_{s,i}w\phi^{V,S}_{v,s-1,i+1}(z,w). \tag{45}$$

Given l and k, positive integers, the factorial moments of order $(l+k)$ are determined from Equation (45) by differentiating repeatedly l times with respect to z and k times with respect to w. Finally, evaluating the resulting expression at $z = w = 1$, we get the equations involving factorial moments of (R^V_p, R^S_p) conditioned to state $(v,s,i) \in \widehat{\mathbb{S}}$ as follows

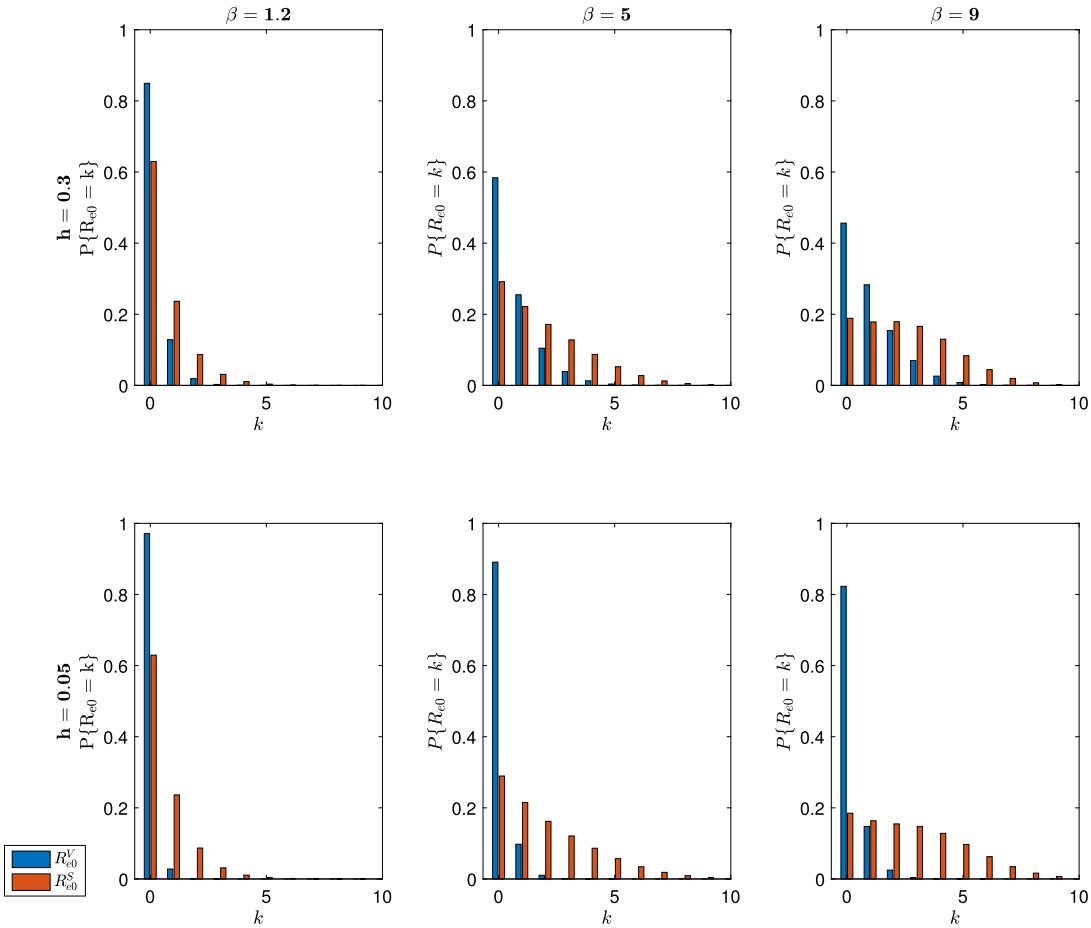

Fig. 2. R^V_{e0} and R^S_{e0} marginal probability mass functions for $\beta \in \{1.2, 5, 9\}$ and $h \in \{0.05, 0.3\}$, when $N = 101$, $\xi = 0.01$, $\gamma = 1$ and for initial state $(50, 50, 1)$.

$$q_{v,s,i} M^{l,k}_{v,s,i} = (1-\delta_{v,0})\eta_{v,i}\left(l M^{l-1,k}_{v-1,s,i+1} + M^{l,k}_{v-1,s,i+1}\right) + (1-\delta_{s,0})\lambda_{s,i}\left(k M^{l,k-1}_{v,s-1,i+1} + M^{l,k}_{v,s-1,i+1}\right). \tag{46}$$

For $1 \le i \le N - v - s$, Equation (46) can be expressed in the matrix form as Equation (44), which concludes the proof. □

Remark 2. Factorial moments of the bi-dimensional vector (R^V_p, R^S_p) can be computed from recursive schemes based on Theorem 4 by applying an analogous procedure to Algorithm 2, with the natural changes in notation and replacing Equation (28) by

$$\mathbf{M}^{l,k}_{v,s} = (\widetilde{\mathbf{A}}_{v,s})^{-1}\Big((1-\delta_{s,0})\mathbf{D}_{v,s}\left(k\widehat{\mathbf{M}}^{l,k-1}_{v,s-1} + \widehat{\mathbf{M}}^{l,k}_{v,s-1}\right) + (1-\delta_{v,0})\mathbf{E}_{v,s}\left(l\widehat{\mathbf{M}}^{l-1,k}_{v-1,s} + \widehat{\mathbf{M}}^{l,k}_{v-1,s}\right)\Big).$$

5. Numerical results

In this Section, we obtain some numerical results to illustrate the theoretical and algorithmic results described in Sections 3 and 4. For all scenarios considered in this section, we have assumed that the population size is $N = 101$, and we have set the time unit as the average infectious period (i.e., $\gamma^{-1} = 1$).

First we focus on the one-dimensional probability distributions of R^V_{e0} and R^S_{e0}. In Fig. 2, we plot histograms for each marginal distribution as we vary the contact rate $\beta \in \{1.2, 5, 9\}$ and the vaccine failure probability $h \in \{0.05, 0.3\}$, assuming that initial vaccine coverage is 50% ($v_0 = 50$) and the external contact rate is $\xi = 0.01$. The height bars correspond to the probability that the index case causes k infections within the vaccinated (blue bars) or within susceptible (red bars) pool. Note that the support of R^V_{e0} and also of R^S_{e0} consists of $\{0, 1, 2, \ldots, 50\}$, but we plot the probability mass functions up to the maximum value of k which accumulates 95% of the probability.

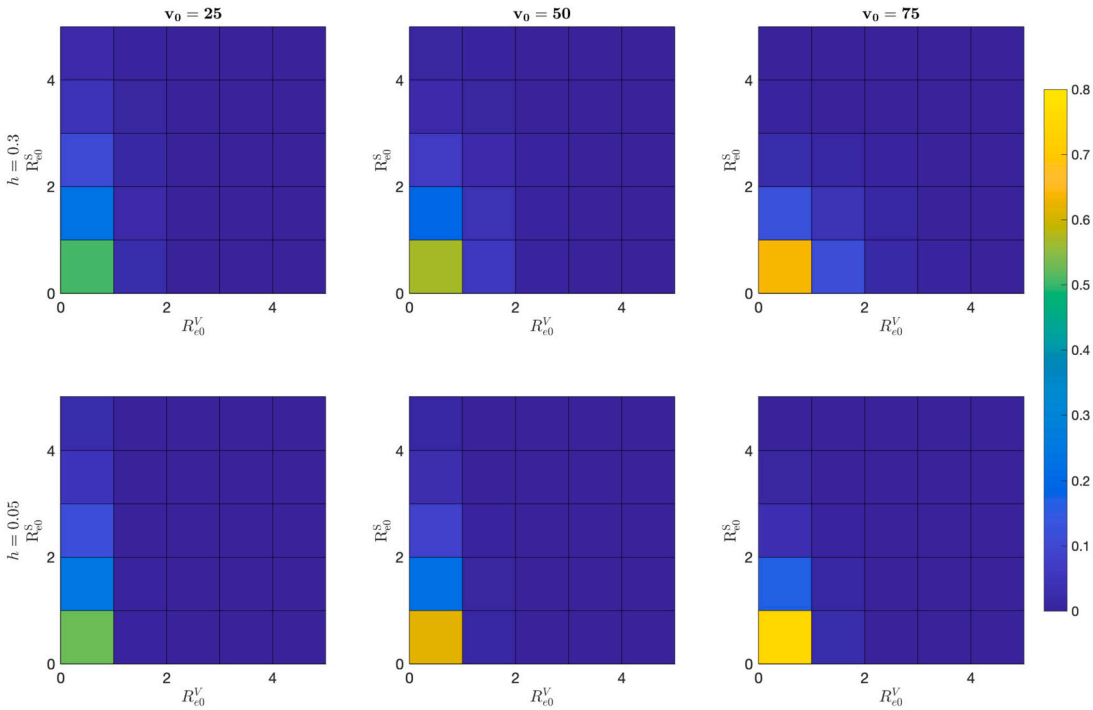

Fig. 3. Joint mass probability distribution function of (R^V_{e0}, R^S_{e0}) for $h \in \{0.05, 0.3\}$, $v_0 \in \{25, 50, 75\}$ and initial state $(v_0, N - v_0 - 1, 1)$, when $N = 101$, $\beta = 1.2$, $\xi = 0.01$ and $\gamma = 1$.

Both distributions are right-skewed and present a decreasing shape for increasing values of k, where larger numbers of infections become more likely as we increase the contact rate β. Regarding vaccine efficacy, we observe a different behaviour for the two pools. For R^V_{e0}, when the vaccine is 70% effective ($h = 0.3$), the probability of the index case recovering before infecting any vaccinated person is higher than 0.4 for all values of β considered. However, for a more effective vaccine ($h = 0.05$), the chance is always greater than 0.8, even for a large contact rate such as $\beta = 9$. On the other hand, we observe that changes in vaccine efficacy have small effects on the probability distribution of R^S_{e0}.

In Figs. 3 and 4, we represent the joint probability mass function of (R^V_{e0}, R^S_{e0}), given by probabilities $x^{l,k}_{v_0, N-v_0-1,1}$. We consider support values (l, k) varying in the grid of integer points $\{0, \dots, a\} \times \{0, \dots, a\}$ which accumulates the 95% of the probability. We compare mass functions for vaccine efficacy $h \in \{0.05, 0.3\}$ and initial vaccine coverage $v_0 \in \{25, 50, 75\}$, when $N = 101$, $\xi = 0.01$ and $\gamma = 1$. Additionally, the contact rate is $\beta = 1.2$ in Fig. 3 and $\beta = 9$ in Fig. 4. Colour plots in both figures show that the most likely event is that the index case does not infect any other individual, with the associate probability increasing as either the vaccine initial coverage v_0 or the vaccine efficacy $1 - h$ is increased. We note that increasing the contact rate β increases the chance that the index case will spread the infection within the population, causing more infections in the susceptible pool than among vaccinated individuals.

Next, we focus on the average number of infections directly caused by the index case within both pools. Our aim is to analyse the influence of the model parameters on these averages. In Fig. 5, we present colour plots for $E[R^V_{e0}]$ (six bottom plots) and $E[R^S_{e0}]$ (top plots), as functions of β and h, for different values of the external contact rate ξ and initial vaccine coverage v_0.

Both expected values increase with increasing values of the internal contact rate β, as one would expect. Under low vaccine coverage (i.e., $v_0 \leq 50$), the probability of vaccine failure has little effect on these averages. We note that when the external rate takes large values (e.g., $\xi = 1$) expected values $E[R^V_{e0}]$ and $E[R^S_{e0}]$ are lower compared to situations where $\xi = 0.01$. This reflects that the index case has fewer opportunities to transmit the disease within each of the pools, due to external infections occurring more often. For increasing values of the vaccine coverage, and decreasing values of external contact rate, the average number of infections caused by the index case in the vaccinated pool, $E[R^V_{e0}]$, increases. On the other hand, due to the constant population size, increasing vaccine coverage leads to a decrease in $E[R^S_{e0}]$. It can be observed that, with the exception of scenarios characterized by high vaccine coverage (e.g., $v_0 = 75$) and substantial vaccine failure probability (e.g., $h = 0.3$), the expected number of infections among susceptible individuals is consistently greater than that among vaccinated individuals.

In Table 1, we display summary statistics: expected values, standard deviations and coefficients of variation of R^V_{e0} and R^S_{e0}, for $\beta \in \{1.2, 5, 9\}$ and $h \in \{0.05, 0.3\}$, when $\xi = 0.01$, $v_0 = s_0 = 50$ and a single initial infected individual in the population. For all scenarios, expected values and standard deviations for R^S_{e0} are greater than their counterpart measures for R^V_{e0}, due to the protection conferred by the vaccine. On the contrary, the coefficient of variation is greater for the variable R^V_{e0} in every case. Hence, R^S_{e0} is more concentrated around its expected value $E[R^S_{e0}]$ than R^V_{e0} around its respective mean value. The expected transmission and standard

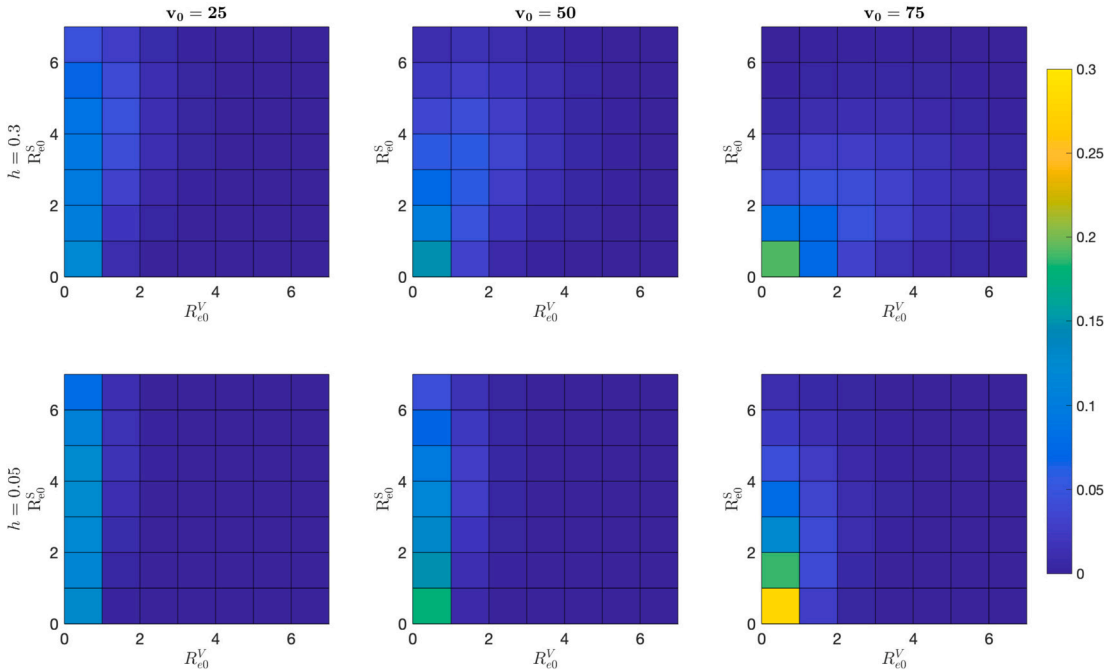

Fig. 4. Joint mass probability distribution function of (R^V_{e0}, R^S_{e0}) for $h \in \{0.05, 0.3\}$, $v_0 \in \{25, 50, 75\}$ and initial state $(v_0, N - v_0 - 1, 1)$, when $N = 101$, $\beta = 9$, $\xi = 0.01$ and $\gamma = 1$.

Table 1
Summary statistics for R^V_{e0} and R^S_{e0}.

β	h	$E[R^V_{e0}]$	$\sigma[R^V_{e0}]$	$CV[R^V_{e0}]$	$E[R^S_{e0}]$	$\sigma[R^S_{e0}]$	$CV[R^S_{e0}]$
1.2	0.05	0.0297	0.1746	5.8788	0.5764	0.9323	1.6175
5	0.05	0.1219	0.3680	3.0189	2.0071	2.0218	1.0073
9	0.05	0.2120	0.4992	2.3547	2.7623	2.2155	0.8020
1.2	0.30	0.1764	0.4532	2.5692	0.5746	0.9285	1.6159
5	0.30	0.6592	0.9701	1.4716	1.8783	1.8461	0.9829
9	0.30	0.9624	1.1531	1.1982	2.4644	1.9495	0.7911

deviation, on both vaccinated and susceptible individuals, increase when the internal contact rate increases. When fixing the internal contact rate, more effective vaccines decrease both $E[R^V_{e0}]$ and $\sigma[R^V_{e0}]$.

Next, we derive analogous numerical analysis for the joint random variable (R^V_p, R^S_p). In particular, Fig. 6 and 7 represent the joint probability mass distributions of (R^V_p, R^S_p) for $\beta = 1.2$ and $\beta = 9$, respectively, for $v_0 \in \{25, 50, 75\}$ and for $h \in \{0.05, 0.3\}$. The behaviour of these distributions is similar to that observed in Fig. 3 and 4, but we notice that a larger region of the support is required to accumulate 95% of the probability distribution of (R^V_p, R^S_p) compared to that of (R^V_{e0}, R^S_{e0}). This observation aligns with intuition, as the distribution of interest accounts for infections caused not only by the index case, but also subsequent transmissions events.

In Fig. 8, we represent the expected value $E[R^S_p]$ (top of the figure) and $E[R^V_p]$ (bottom of the figure) as a function of the internal transmission rate β, and the vaccine failure probability h, for vaccine coverages $v_0 \in \{25, 50, 75\}$ and external contact rates $\xi \in \{0.01, 1\}$. The expected number of infections among susceptible individuals caused by all the infective individuals prior to the first recovery is greater than among vaccinated individuals, especially for lower vaccine failure probabilities, showing the importance of the vaccine. On the other hand, when considering large vaccine coverage (e.g.; $v_0 \geq 75$) and external contact rates (e.g.; $\xi = 1$), we observe $E[R^S_p] < E[R^V_p]$ for internal contact rates greater than 7.8, in combination with significant vaccine failure probability $h = 0.3$. Overall, the effect of the internal contact rate β and the vaccine failure probability h on $E[R^S_p]$ and $E[R^V_p]$ is similar to Fig. 5.

In contrast to Fig. 5, large external contact rates ξ (e.g.; $\xi = 1$) lead to greater values of $E[R^V_p]$ and $E[R^S_p]$. This behaviour is intuitive because when external transmission rates are high, there is a greater number of infections among susceptible and vaccinated individuals, resulting in a larger average number of infections produced by the infected individuals in the population. Increasing vaccine coverage leads to higher values of $E[R^V_p]$ since there are more vaccinated individuals in the population. Conversely, increasing vaccine coverage results in smaller values of $E[R^S_p]$ for the similar reasons. The effect of the vaccine efficacy for large/small vaccines coverages is as the stated in Fig. 5.

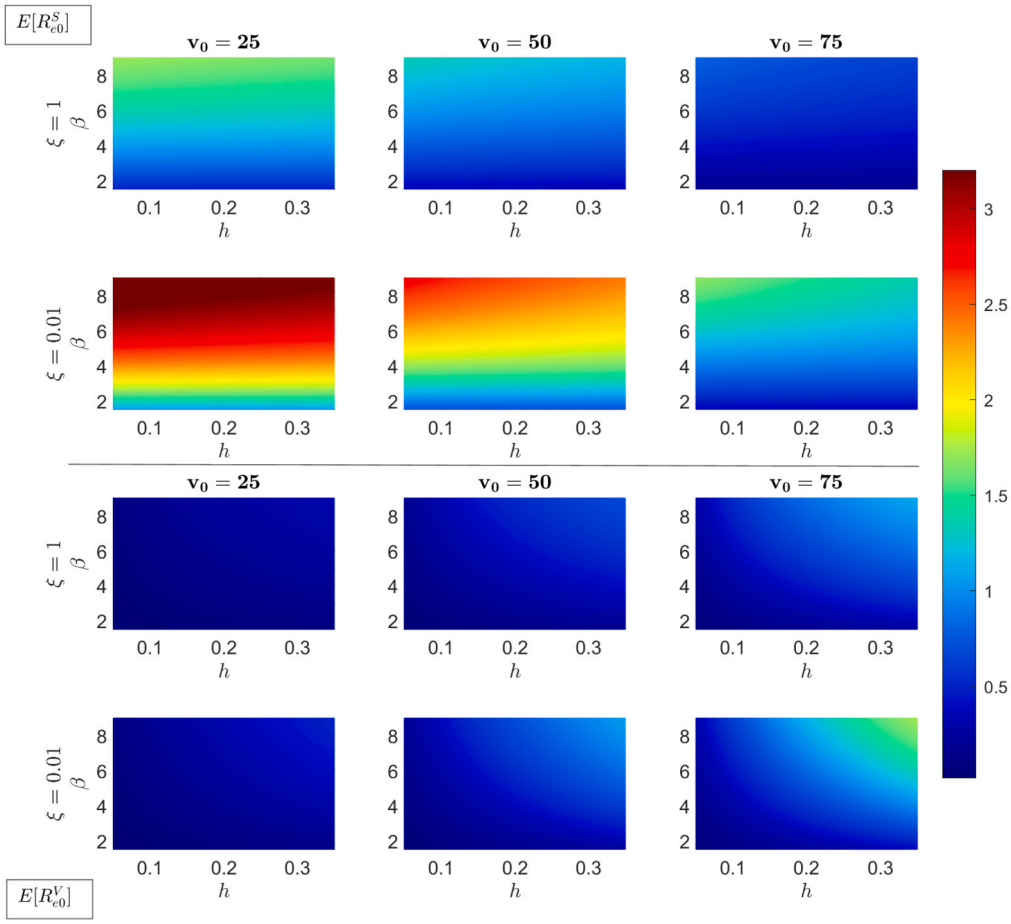

Fig. 5. $E[R^V_{e0}]$ and $E[R^S_{e0}]$ as a function of β and h, for different values of ξ and v_0.

Table 2
Summary statistics for R^V_p and R^S_p.

β	h	$E[R^V_p]$	$\sigma[R^V_p]$	$CV[R^V_p]$	$E[R^S_p]$	$\sigma[R^S_p]$	$CV[R^S_p]$
1.2	0.05	0.0466	0.2189	4.6974	0.9196	1.1860	1.2897
5	0.05	0.1350	0.3882	2.8756	2.5751	2.7818	1.0803
9	0.05	0.2307	0.5281	2.2891	4.2509	4.2596	1.0020
1.2	0.30	0.2727	0.5632	2.0653	0.8995	1.1725	1.3035
5	0.30	0.7935	1.1504	1.4498	2.5547	2.7710	1.0847
9	0.30	1.3482	1.7108	1.2690	4.2333	4.2520	1.0044

In Table 2, we record some summary statistics of interest of the variables R^V_p and R^S_p. In particular we show the mean, standard deviation and coefficient of variation of these variables for $\beta \in \{1.2, 5, 9\}$ and $h \in \{0.05, 0.3\}$, when $\xi = 0.01$, $v_0 = s_0 = 50$ and there is a single initial infected individual in the population. As expected, average values and standard deviations are greater for R^S_p than for R^V_p due to the protection that the vaccine confers. In contrast, we obtain greater coefficient of variations for R^V_p than for R^S_p for the same reasons explained in Table 1. The impact on these summary statistics of the internal contact rate and the vaccine failure probability is similar to that observed in Table 1.

5.1. Case study: influenza in a boarding school

We focus here on a particular case study, related to the spread of influenza in a school, in order to illustrate our methodology. In this context, we will examine the variables R_{e0} and R_p, to gain further insights into the epidemic dynamics.

Influenza, commonly known as the flu, is a highly contagious respiratory illness caused by influenza viruses. The symptoms can range from mild, such as fever, cough, sore throat, body aches, and fatigue, to severe complications like pneumonia and respiratory failure. Particularly vulnerable populations, such as young children, the elderly and individuals with underlying health conditions, face an increased risk of hospitalisation and, tragically, even death. The virus spreads easily through respiratory droplets when an

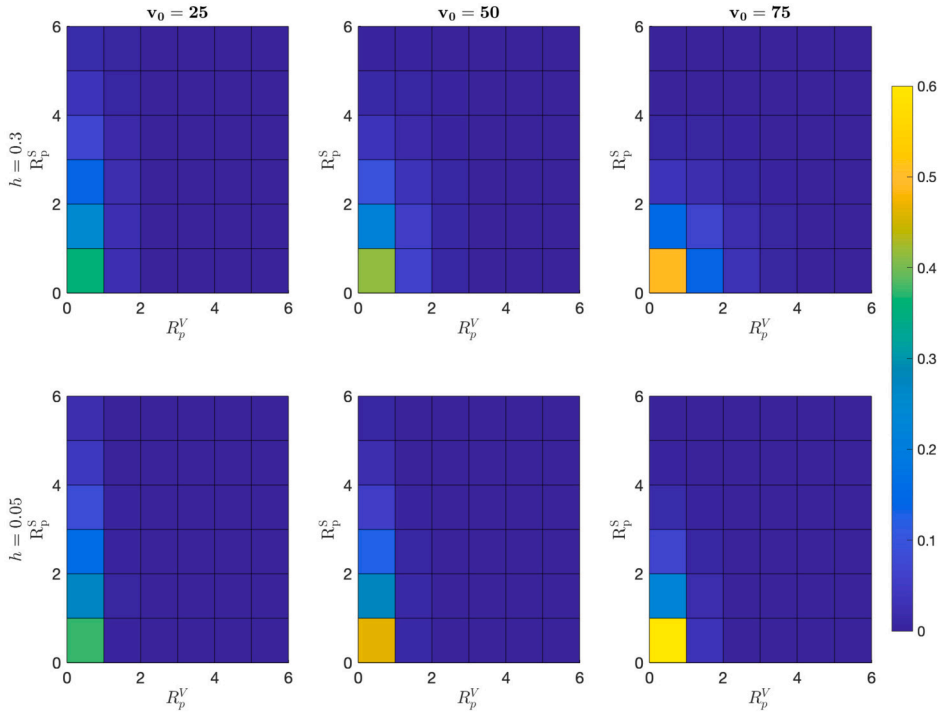

Fig. 6. Joint probability mass distribution function of (R_p^V, R_p^S) for several values of h and vaccination levels (v_0) in a population of $N = 101$ individuals, with an initial infective individual, $\beta = 1.2$, $\gamma = 1$ and $\xi = 0.01$.

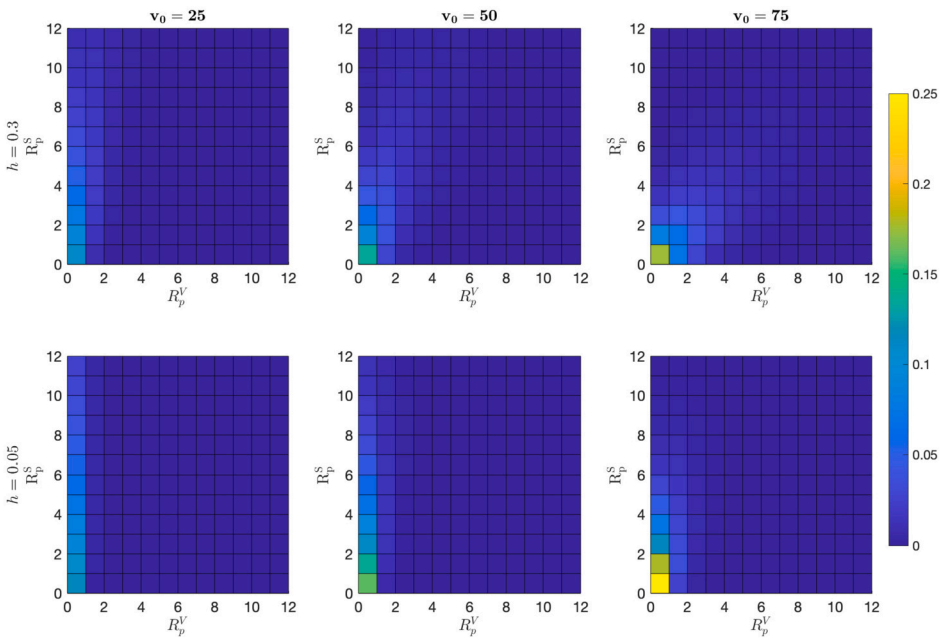

Fig. 7. Joint probability mass distribution function of (R_p^V, R_p^S) for several values of h and vaccination levels (v_0) in a population of $N = 101$ individuals, with an initial infective individual and $\beta = 9$, $\gamma = 1$ and $\xi = 0.01$.

infected person coughs, sneezes, or talks, making person-to-person transmission common. Although vaccines exist for this pathogen, which need to be annually updated depending on the circulating strains, they are imperfect. Nevertheless, vaccination remains a crucial tool in mitigating the spread of this infectious disease every year, and reducing its impact on public health.

In January 1978, an influenza outbreak occurred in a boarding school located in the north of England, which was documented in a report published in the British Medical Journal [40]. Data from this outbreak were analyzed in [41] and [42]. For our analysis, we

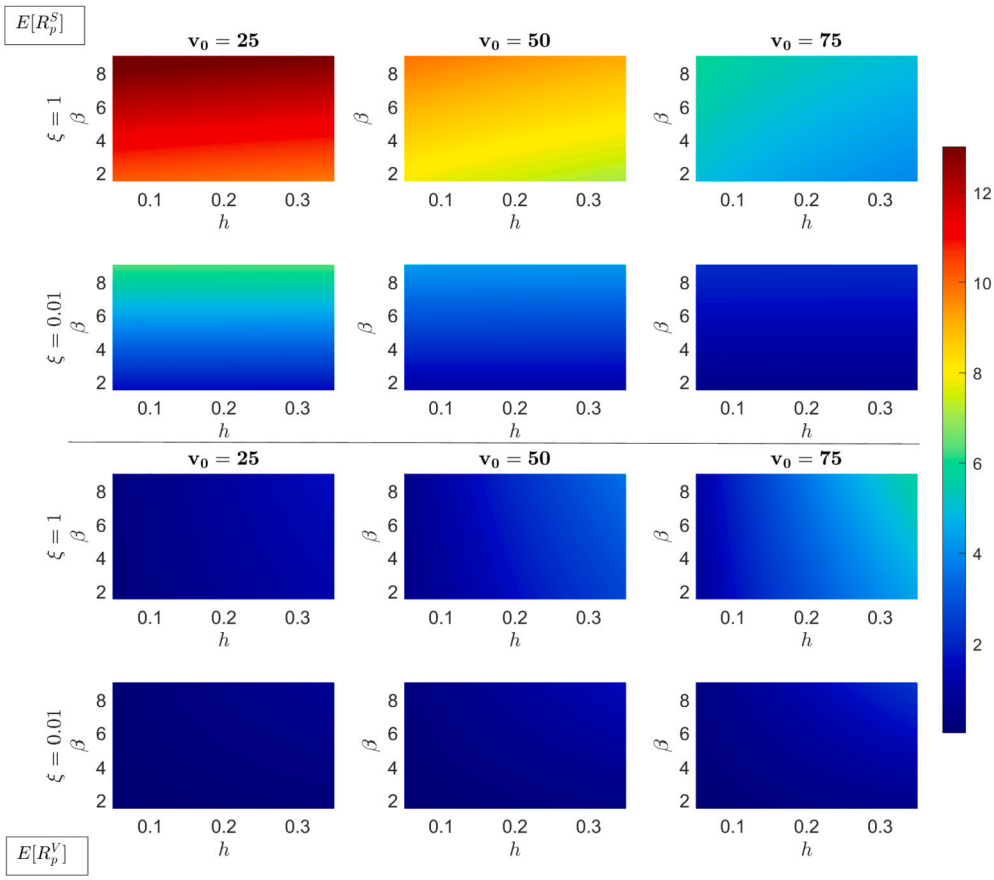

Fig. 8. $E[R_p^S]$ and $E[R_p^V]$ as a function of β and h. Different scenarios arise in a population of $N = 101$ individuals, with an initial infectious individual and $\gamma = 1$ when $v_0 \in \{25, 50, 75\}$ and $\xi \in \{0.01, 1\}$.

Table 3
Influenza in a boarding school. Summary statistics for R_{e0}^V and R_{e0}^S.

v_0	$E[R_{e0}^V]$	$\sigma[R_{e0}^V]$	$CV[R_{e0}^V]$	$E[R_{e0}^S]$	$\sigma[R_{e0}^S]$	$CV[R_{e0}^S]$
30	0.3721	0.6793	1.8255	2.0346	2.0326	0.9990
60	0.7686	1.0986	1.4293	1.2300	1.4467	1.1761
90	1.1836	1.5281	1.2910	0.3230	0.6154	1.9052

draw upon the parameters derived from these studies where the average infectious period was found to be $1/\gamma = 2.2$ days and the transmission rate $\beta = 1.66$. Consequently, the calculated basic reproduction number, defined as $R_0 = \beta/\gamma$, was 3.652 for this influenza strain during this outbreak. In evaluating vaccine effectiveness, we refer to [43], where influenza vaccination was shown to provide increased protection in fully vaccinated children, with an effectiveness rate of 61.79% ($95\% CI : 54.45 - 69.13$). Consequently, we adopt a vaccine failure probability of $h = 0.3821$ here. Additionally, an external infection rate of $\xi = 0.01$ is considered for illustrative purposes.

In Table 3, we provide a comprehensive overview of the statistics, including expected values, standard deviations, and coefficients of variation for the marginal random variables R_{e0}^V and R_{e0}^S. The analysis relates to the scenario described in the previous paragraph. It considers different levels of vaccine coverage, namely $v_0 \in \{30, 60, 90\}$. These values represent low, medium and high vaccination coverage within the boarding school.

As we increase vaccination coverage, we observe a corresponding increase in the number of vaccinated individuals who become infected. This is because there are more vaccinated individuals than susceptible ones in the population. However, the crucial role of vaccination becomes clear when, for instance, we reach a 60% vaccination coverage. At this level, the average number of infections in susceptible individuals is significantly higher than in vaccinated individuals. Even at 90% coverage, susceptible individuals continue to get infected. As vaccination coverage increases, the coefficient of variation for the average number of infections inside the vaccinated group decreases. In contrast, this behaviour is reversed for susceptible individuals, where the coefficient of variation increases with increasing vaccination coverage. This observation highlights the importance of vaccination in shaping infection dynamics and demonstrates its efficacy even in high vaccine failure scenarios.

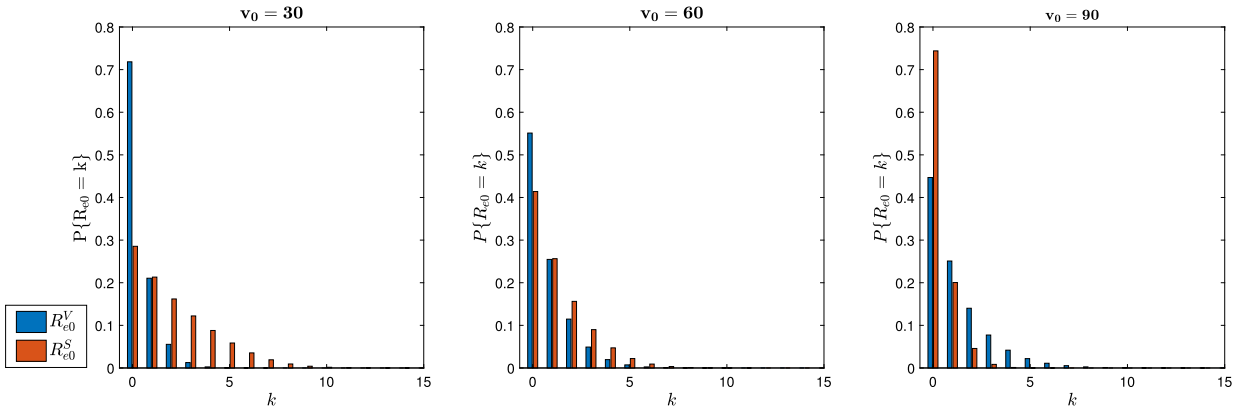

Fig. 9. Influenza in a boarding school. R^V_{e0} and R^S_{e0} marginal probability mass functions for $R_0 = 3.652$, $\xi = 0.01$ and $h = 0.3821$, when $N = 101$ and for $v_0 \in \{30, 60, 90\}$.

Table 4
Influenza in a boarding school. Summary statistics for R^V_p and R^S_p.

v_0	$E[R^V_p]$	$\sigma[R^V_p]$	$CV[R^V_p]$	$E[R^S_p]$	$\sigma[R^S_p]$	$CV[R^S_p]$
30	0.4570	0.7885	1.7253	2.7277	2.9297	1.0740
60	0.9258	1.2726	1.3745	1.5786	1.8619	1.1794
90	1.4132	1.7387	1.2303	0.4015	0.7071	1.7611

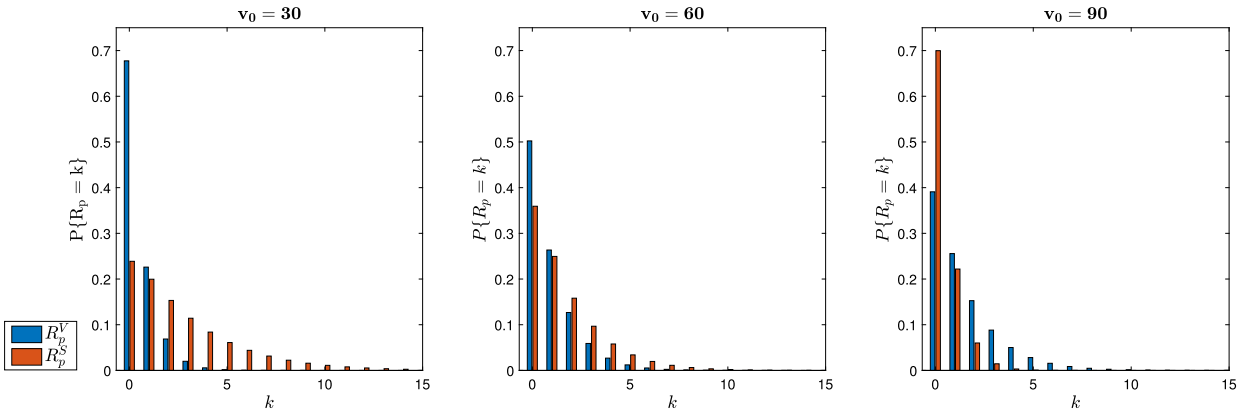

Fig. 10. Influenza in a boarding school. R^V_p and R^S_p marginal probability mass functions for $R_0 = 3.652$, $\xi = 0.01$ and $h = 0.3821$, when $N = 101$ and for $v_0 \in \{30, 60, 90\}$.

In Fig. 9, R^V_{e0} and R^S_{e0} mass functions are plotted when vaccine coverage v_0 varies in the set $\{30, 60, 90\}$. The objective is to compare the epidemic patterns as we increase the vaccination coverage. The height of the bars corresponds to the probability that the index case causes k infections within vaccinated pool (blue bars) or susceptible pool (red bars). Probability mass functions are plotted up to the maximum value k that accumulates 95% of the probability.

Both probability distributions exhibit a right-skewed pattern, indicating a decreasing trend as the number of cases, k, increases. Regarding the distribution for the number of secondary cases generated by the index case in vaccinated individuals, we observe that most of the probability is concentrated in the initial mass points and, as vaccination coverage increases, the slope of the distribution becomes less steep. It is important to note that the behaviour of the variable R^S_{e0} is opposite to this pattern, showing a trend that is inverse as vaccination coverage increases.

Finally, in Table 4 and Fig. 10, R^S_p and R^V_p show a similar behaviour to that observed for R^S_{e0} and R^V_{e0} when focusing on the corresponding summary statistics and probability distributions, but with larger averages, as expected.

6. Conclusions

This paper deals with a stochastic SIR-type model. An external source of infection is considered and vaccination as a health control measure is considered. A three-dimensional continuous-time Markov chain is used to model the evolution of an infectious disease within a small-to-moderate size population.

Our interest is in quantifying the spread of this epidemic process by analysing the number of infections produced either by a selected infectious individual or by the whole infectious group during a time interval that depends on individual recovery times. Our main contribution is to adapt exact reproduction numbers, R_{e0} and R_p, to quantify the potential transmission of the epidemic by distinguishing whether new infections occur among individuals in the susceptible or vaccinates pools.

This bi-dimensional study can be used to better understand the effect of vaccination on the spread of a pathogen. In addition, recursive schemes derived from Algorithms 1 and 2, and Remarks 1 and 2 allow us to compute some joint characteristics of the involved bi-dimensional vectors. Through a detailed analysis, we have determined the exact orders of complexity of both algorithms [44]. They can be described in terms of $\Theta((v_0 s_0)^2)$ and $\Theta(v_0 s_0)$ for Algorithm 1 and 2, respectively. These results are presented under the assumption that the Thomas Algorithm (TA) has been employed for the inversion of matrices. The TA is particularly suitable and efficient for tri-diagonal systems of equations. Complexity results highlight the fundamental relationship between the algorithm's execution time and the size of the population; and more specifically the initial number of susceptible and vaccinated individuals. We have illustrated our methodology with numerical examples, implemented in Matlab software, by analyzing the dependencies between each marginal random variable of (R_{e0}^V, R_{e0}^S) and (R_p^V, R_p^S).

The results highlight the critical role of vaccination strategies in controlling the spread of the infection. The interactions between parameters reveal the complexity of disease dynamics and emphasise the need for tailored vaccination policies in real-world scenarios. Furthermore, internal and external contact rates, β and ξ, play a key role in influencing the probability of infection and need to be considered in epidemiological modelling. The analysis emphasises the importance of vaccine efficacy and coverage, providing valuable insights for public health interventions.

For future work, this investigation can be continued in other directions by considering additional assumptions about infectious disease dynamics, such as a latency period and waning vaccines, which more realistically reflect the characteristics of a vaccine-preventable disease.

Data availability

No data was used for the research described in the article.

Acknowledgement

The authors would like to thank the referees for their helpful comments and useful suggestions which greatly improved the paper. Special thanks are due to Prof. C. Pareja, Faculty of Statistical Studies, Complutense University of Madrid, for his contribution and guidance in the determination of the precise orders of algorithmic complexity. We greatly appreciate his generosity in sharing his expertise and knowledge in this area. This research has been made possible by the support of the Ministry of Science and Innovation (Government of Spain) through project PID2021-125871NB-I00. The first author also expresses gratitude to the British Spanish Society for their financial support through a BBS 2021 award, which has facilitated the development of this research.

References

[1] C. Thèves, E. Crubézy, P. Biagini, History of smallpox and its spread in human populations, Microbiol. Spectr. 4 (4) (2016), https://doi.org/10.1128/microbiolspec.PoH-0004-2014.
[2] E.P. Chevalier-Cottin, H. Ashbaugh, N. Brooke, G. Gavazzi, M. Santillana, N. Burlet, M. Tin Tin Htar, Communicating benefits from vaccines beyond preventing infectious diseases, Infect. Dis. Ther. 9 (2020) 467–480, https://doi.org/10.1007/s40121-020-00312-7.
[3] F.E. Andre, R. Booy, H.L. Bock, J. Clemens, S.K. Datta, T.J. John, B.W. Lee, S. Lolekha, H. Peltola, T.A. Ruff, M. Santosham, H.J. Schmitt, Vaccination greatly reduces disease, disability, death and inequity worldwide, Bull. World Health Organ. 86 (2) (2008) 140–146, https://doi.org/10.2471/blt.07.040089, PMID: 18297169; PMCID: PMC2647387.
[4] M. Gamboa, M.J. Lopez-Herrero, The effect of setting a warning vaccination level on a stochastic SIVS model with imperfect vaccine, Mathematics 8 (7) (2020) 1136, https://doi.org/10.3390/math8071136.
[5] X. Meng, L. Chen, The dynamics of a new SIR epidemic model concerning pulse vaccination strategy, Appl. Math. Comput. 197 (2) (2008) 582–597, https://doi.org/10.1016/j.amc.2007.07.083.
[6] O.D. Makinde, Adomian decomposition approach to a SIR epidemic model with constant vaccination strategy, Appl. Math. Comput. 184 (2) (2007) 842–848, https://doi.org/10.1016/j.amc.2006.06.074.
[7] U. Wiedermann, E. Garner-Spitzer, A. Wagner, Primary vaccine failure to routine vaccines: why and what to do?, Hum. Vaccines Immunother. 12 (1) (2016) 239–243, https://doi.org/10.1080/21645515.2015.1093263.
[8] X. Liu, T. Yasuhiro, I. Shingo, SVIR epidemic models with vaccination strategies, J. Theor. Biol. 253 (1) (2008) 1–11, https://doi.org/10.1016/j.jtbi.2007.10.014.
[9] J. Arino, C.C. McCluskey, P. van den Driessche, Global results for an epidemic model with vaccination that exhibits backward bifurcation, SIAM J. Appl. Math. 64 (2003) 260–276, https://doi.org/10.1137/S0036139902413829.
[10] J. Arino, C. Sun, W. Yan, Global analysis for a general epidemiological model with vaccination and varying population, J. Math. Anal. Appl. 372 (2010) 208–223, https://doi.org/10.1016/j.jmaa.2010.07.017.
[11] F. Ball, D. Sirl, Acquaintance vaccination in an epidemic on a random graph with specified degree distribution, J. Appl. Probab. 50 (2013) 1147–1168, https://doi.org/10.1239/jap/1389370105.
[12] F. Ball, D. Sirl, Evaluation of vaccination strategies for SIR epidemics on random networks incorporating household structure, J. Math. Biol. 76 (2018) 483–530, https://doi.org/10.1007/s00285-017-1139-0.
[13] C.M. Kribs-Zaleta, M. Martcheva, Vaccination strategies and backward bifurcation in an age-since-infection structured model, Math. Biosci. 177 (2002) 317–332, https://doi.org/10.1016/S0025-5564(01)00099-2.
[14] W. Li, Q. Zhang, Construction of positivity-preserving numerical method for stochastic SIVS epidemic model, Adv. Differ. Equ. 219 (2019) 25, https://doi.org/10.1186/s13662-019-1966-y.
[15] M. Iannelli, M. Martcheva, X.Z. Li, Strain replacement in an epidemic model with super-infection and perfect vaccination, Math. Biosci. 195 (2005) 23–46, https://doi.org/10.1016/j.mbs.2005.01.004.

[16] M.E. Alexander, C. Bowman, S.M. Moghadas, R. Summers, A.B. Gumel, B.M. Sahai, A vaccination model for transmission dynamics of influenza, SIAM J. Appl. Dyn. Syst. 3 (2004) 503–524, https://doi.org/10.1137/030600370.
[17] F. Ball, P.D. O'Neill, J. Pike, Stochastic epidemic models in structured populations featuring dynamic vaccination and isolation, J. Appl. Probab. 44 (2007) 571–585, https://doi.org/10.1239/jap/1189717530.
[18] Y. Lin, D. Jiang, S. Wang, Stationary distribution of a stochastic SIS epidemic model with vaccination, Physica A 394 (2014) 187–197, https://doi.org/10.1016/j.physa.2013.10.006.
[19] Y. Guo, Stochastic regime switching SIS epidemic model with vaccination driven by Lévy noise, Adv. Differ. Equ. (2017) 1–15, https://doi.org/10.1186/s13662-017-1424-7.
[20] J.C. Eckalbar, W.L. Eckalbar, Dynamics of an SIR model with vaccination dependent on past prevalence with high-order distributed delay, Biosystems 129 (2015) 50–65, https://doi.org/10.1016/j.biosystems.2014.12.004.
[21] I. Abouelkheir, F. El Kihal, M. Rachik, I. Elmouki, Optimal impulse vaccination approach for an SIR control model with short-term immunity, Mathematics 7 (2019) 420, https://doi.org/10.3390/math7050420.
[22] S.M. Moghadas, Modelling the effect of imperfect vaccines on disease epidemiology, Discrete Contin. Dyn. Syst., Ser. B 4 (2004) 999–1012, https://doi.org/10.3934/dcdsb.2004.4.999.
[23] X. Wang, D. Jia, S. Gao, C. Xia, X. Li, Z. Wang, Vaccination behavior by coupling the epidemic spreading with the human decision under the game theory, Appl. Math. Comput. 380 (2020) 125232, https://doi.org/10.1016/j.amc.2020.125232.
[24] M. Safan, F.A. Rihan, Mathematical analysis of an SIS model with imperfect vaccination and backward bifurcation, Math. Comput. Simul. 96 (2014) 195–206, https://doi.org/10.1016/j.matcom.2011.07.007.
[25] A.B. Gumel, S.M. Moghadas, A qualitative study of a vaccination model with non-linear incidence, Appl. Math. Comput. 143 (2–3) (2003) 409–419, https://doi.org/10.1016/S0096-3003(02)00372-7.
[26] Y. Zhao, J. Daqing, The threshold of a stochastic SIS epidemic model with vaccination, Appl. Math. Comput. 243 (2014) 718–727, https://doi.org/10.1016/j.amc.2014.05.124.
[27] J.R. Artalejo, A. Economou, M.J. Lopez-Herrero, The maximum number of infected individuals in SIS epidemic models: computational techniques and quasi-stationary distributions, J. Comput. Appl. Math. 233 (10) (2010) 2563–2574, https://doi.org/10.1016/j.cam.2009.11.003.
[28] M. Gamboa, M.J. Lopez-Herrero, Measuring infection transmission in a stochastic SIV model with infection reintroduction and imperfect vaccine, Acta Biotheor. (2020) 1–26, https://doi.org/10.1007/s10441-019-09373-9.
[29] D. Kiouach, L. Boulaasair, Stationary distribution and dynamic behaviour of a stochastic SIVR epidemic model with imperfect vaccine, J. Appl. Math. (2018), https://doi.org/10.1155/2018/1291402.
[30] A. El Koufi, J. Adnani, A. Bennar, N. Yousfi, Analysis of a stochastic SIR model with vaccination and nonlinear incidence rate, Int. J. Differ. Equ. (2019), https://doi.org/10.1155/2019/9275051.
[31] Y. Cheng, Q. Pan, M. He, Psychological and behavioral effects in epidemiological model with imperfect vaccination compartment, Math. Methods Appl. Sci. 38 (2015) 4729–4740, https://doi.org/10.1002/mma.3387.
[32] M. Gamboa, M. López-García, M.J. Lopez-Herrero, A Stochastic SVIR Model with Imperfect Vaccine and External Source of Infection, In Lecture Notes in Computer Science, vol. 13104, Springer Nature, 2021.
[33] J.R. Artalejo, M.J. Lopez-Herrero, On the exact measure of disease spread in stochastic epidemic models, Bull. Math. Biol. 75 (7) (2013) 1031–1050, https://doi.org/10.1007/s11538-013-9836-3.
[34] D. Posny, J. Wang, Computing the basic reproductive numbers for epidemiological models in non homogeneous environments, Appl. Math. Comput. 242 (2014) 473–490, https://doi.org/10.1016/j.amc.2014.05.079.
[35] Y. Cai, J. Jiao, Z. Gui, Y. Liu, W. Wang, Environmental variability in a stochastic epidemic model, Appl. Math. Comput. 329 (2018) 210–226, https://doi.org/10.1016/j.amc.2018.02.009.
[36] Y. Cai, Y. Kang, W. Wang, A stochastic SIRS epidemic model with nonlinear incidence rate, Appl. Math. Comput. 305 (2017) 221–240, https://doi.org/10.1016/j.amc.2017.02.003.
[37] X. Duan, S. Yuan, X. Li, Global stability of an SVIR model with age of vaccination, Appl. Math. Comput. 226 (2014) 528–540, https://doi.org/10.1016/j.amc.2013.10.073.
[38] Y. Lin, D. Jiang, P. Xia, Long-time behavior of a stochastic SIR model, Appl. Math. Comput. 236 (2014) 1–9, https://doi.org/10.1016/j.amc.2014.03.035.
[39] J.V. Ross, Invasion of infectious diseases in finite homogeneous populations, J. Theor. Biol. 289 (2011) 83–89, https://doi.org/10.1016/j.jtbi.2011.08.035.
[40] Anon, Epidemiology: influenza in a boarding school, Br. Med. J. 4 (1978).
[41] M.J. Keeling, P. Rohani, Modeling Infectious Diseases in Humans and Animals, Princeton University Press, 2008.
[42] J.V. Ross, D.E. Pagendam, P.K. Pollett, On parameter estimation in population models II: multi-dimensional processes and transient dynamics, Theor. Popul. Biol. 75 (2–3) (2009) 123–132, https://doi.org/10.1016/j.tpb.2008.12.002.
[43] M. Kalligeros, F. Shehadeh, E.K. Mylona, C. Dapaah-Afriyie, R. van Aalst, A. Chit, E. Mylonakis, Influenza vaccine effectiveness against influenza-associated hospitalization in children: a systematic review and meta-analysis, Vaccine 38 (14) (2020) 2893–2903, https://doi.org/10.1016/j.vaccine.2020.02.049.
[44] C.A. Shaffer, A Practical Introduction to Data Structures and Algorithm Analysis, Prentice Hall, Upper Saddle River, NJ, 1997.